Technical Note

Plasmon-Enhanced Four-Wave Mixing Imaging for Microdroplet-based Single-cell Analysis

Lili Cong, Yijia Geng, Yu Tian, Zepeng Huo, Dianshuai Huang, Chongyang Liang, Weiqing Xu, Yuling Wang, and Shuping Xu

Anal. Chem., **Just Accepted Manuscript** • DOI: 10.1021/acs.analchem.0c00816 • Publication Date (Web): 15 Jun 2020

Plasmon-Enhanced Four-Wave Mixing Imaging for Microdroplet-based Single-cell Analysis

Lili Cong[a], *Yijia Geng*[a], *Yu Tian*[a], *Zepeng Huo*[a], *Dianshuai Huang*[b], *Chongyang Liang*[b], *Weiqing Xu*[a], *Yuling Wang*[c], *and Shuping Xu*[*a,c]

[a] State Key Laboratory of Supramolecular Structure and Materials, Institute of Theoretical Chemistry, College of Chemistry, Jilin University 130012 Changchun, China

[b] Institute of Frontier Medical Science, Jilin University 130021 Changchun, China

[c] Department of Molecular Sciences, ARC Centre of Excellence for Nanoscale BioPhotonics (CNBP), Macquarie University, 2109 Sydney, Australia

AUTHOR INFORMATION

Corresponding Author

* State Key Laboratory of Supramolecular Structure and Materials, Institute of Theoretical Chemistry, College of Chemistry, Jilin University

2699 Qianjin Ave. 130012 Changchun, China

E-mail: xusp@jlu.edu.cn

ABSTRACT: A high-throughput single-cell analytical technique based on the microdroplet array integrated with the plasmon-enhanced four-wave mixing (PE-FWM) imaging was developed, which is appliable for the highly sensitive and automatic assessment of the surface receptors of cells. The metal nanoprobes were prepared by simply decorating metal nanoparticles with capturing molecules (antibody or molecules with surface identification function). Owing to the multi-frequency selection of lasers *via* resonating their plasmonic bands, these metal nanoprobes are highly recognizable under the FWM imaging and display high photostability above fluorescent dyes. This PE-FWM imaging technique shows superior to dark-field imaging due to almost no interference from off-resonant species and exhibits the anti-fade feature that is suitable for long-period cell monitoring. The automated processing of images is available for the analysis of cell heterogeneity according to the cell surface receptors. Emerging applications such as single-cell analysis, bioimaging, metabolite, and drug tracing, offer many biological and medical possibilities with broad application prospects.

KEYWORDS. Four-wave mixing imaging, microfluidic droplet, plasmon resonance, metal nanoparticle, single-cell analysis.

Introduction

Single-cell analysis is an interdisciplinary frontier field of analytical chemistry, biology, and medicine. It studies on individual biological cells in a population for identifying differences between cell to cell and elucidating cellular heterogeneity which is shadowed behind population-averaged measurements. Owing to the micron scale of cells, analytical tools for single-cell analysis are usually based on microscopy, microspectroscopy or micromanipulation, for example, flow cytometry (FC),[1] microfluidic system,[2-4] microcapillary electrophoresis system,[5] etc. FC is a single-cell sorting dominating equipment and is an essential tool for single-cell research. It is a scattering intensity/fluorescence intensity-based analytical method and can carry out multi-parameter, fast, and large data quantitative analysis, which has been used for a single cell sorting and screening. At present, this technique has been widely applied in clinical practice, used for the detection of peripheral blood white blood cells, bone marrow cells,

tumor cells, HIV, etc., and has become an indispensable device for *in vitro* diagnosis. Another single-cell analysis device is the droplet microfluidics. It involves the generation of microscale droplets, showing potential in the field of single-cell analysis because it has ultra-high-throughput cell encapsulation for cell sorting.[6] Microdroplets can encapsulate a single cell, providing an independent internal environment, so that the study of a single cell is not disturbed by biological or abiotic factors. In the single-cell analysis, the loss of cell number was avoided in the microdroplet compared with the dispersed cells. In addition, microdroplets can encapsulate a single cell to track a specific cellular change, which flow cytometry cannot achieve. Compared with suspended cells, microdroplets can be used as independent reactors to observe the changes of cells in the droplets in real time. At the same time, the droplet also provides a powerful internal environment for the cell, providing nutrients for the cell in a certain period of time, making the study of a specific living cell level possible.

Four-wave mixing (FWM) is a third-order nonlinear optical effect and shows various forms, e.g. coherent anti-stokes Raman spectroscopic imaging (CARS), two-photon absorption (TPA)-enhanced difference-frequency/sum-frequency mixing, and third-

harmonic generation (THG), etc. Under certain phase-matching conditions, two or three light beams with different wavelengths can produce another light beam. These unique optical phenomena have been widely applied for rapid, label-free imaging of tissue samples, as well as the *in vivo* imaging during surgery, to reveal tumor margins.[7] In 2017, the stimulated Raman scattering (SRS) has been developed for the single-cell analysis. Cheng et al. [8] developed a 32-channel multiplex SRS flow cytometry (SRS-FC) technique that can measure chemical contents of single particles at a speed of 5 μs per Raman spectrum, and they demonstrated the discrimination of polymer beads at a throughput of up to 11,000 particles per second, showing four orders of magnitude improvement in throughput compared to conventional spontaneous Raman flow cytometry. Compared with many cell sorting methods based on the Raman fingerprints or signal intensities,[8] the imaging-based cell sorting can acquire information-rich images at high frame rates, and it developed rapidly and become very useful tools for single-cell analysis.[9] Many unique high-speed imaging methods, e.g. time delay integral imaging, time-coded excitation imaging, frequency division multiplexing imaging, and time-space conversion imaging, etc. were developed to build a snapshot library of multiple cells in a relatively short time, which

are very useful for high-throughput, high-speed flow single-cell analysis.[9] High-content live-cell imaging is also another widely used image-based assay for cell screening and assessment according to image recognition and cluster analysis.[10] Besides various imaging techniques, high sensitive and image contrast probes are necessary and attract more and more researchers.[11]

Metal nanoparticles (MNPs) as one type of classical nanomaterials have been widely used for bio-labels or bio-markers in combination with many sensing approaches and imaging techniques since they can provide large imaging contrast, high detection sensitivity, and good biocompatibility. FWM effects can be effectively enhanced by the localized surface plasmon resonance (LSPR) effect of metal nanoparticles (MNPs).[12,13] These plasmonic nanoparticle-based nanoprobes have also been developed for FWM imaging of cells,[14] Golgi structures[15] and monitoring the dynamics of cellular physiological processes.[16] However, so far, this unique optical amplification phenomenon has not been used in the field of high-throughput single-cell analysis yet.

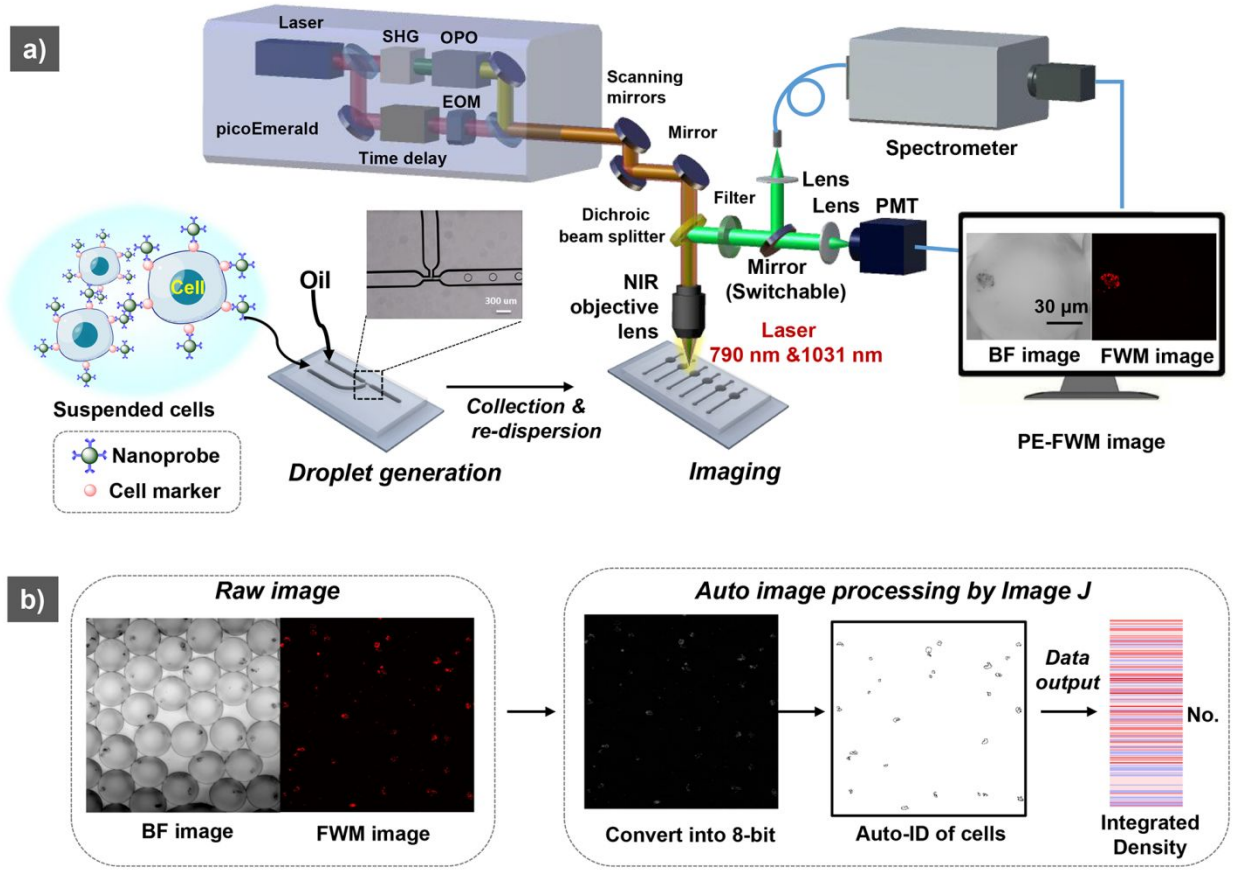

Scheme 1. a) The work flow for detecting cell markers [epidermal growth factor receptor (EGFR) and sialic acid (SA)] on a single living cell by the PE-FWM microdroplet platform with the help of the plasmon-based nanoprobe. b) The process of automatic image processing by Image J software.

The current study is the first report to investigate single-cell imaging analysis in microdroplets by using the improved FWM signal of metal nanoprobes. The microdroplet can protect the cell from the interference from neighboring cells or the surrounding environments.

A universal strategy for fabricating the plasmon-based FWM nanoprobes was adopted (**Scheme S1**) by simple surface decorations of MNPs with capturing molecules (**Figure S1**).[17,18] Since MNPs are highly recognizable under PE-FWM imaging due to the multi-frequency selection *via* resonating the localized surface plasmon bands of MNPs, these nanoprobes showed an extremely high FWM image contrast relative to the off-resonant species (e.g. glass slide, oil phase, polydimethylsiloxane, surfactants, and cells as well). With the assistance of these nanoprobes, the FWM imaging of the cell-encapsulated microdroplet arrays was completed and the cell-to-cell difference was disclosed by the over-expressed biomarkers [epidermal growth factor receptor (EGFR) and sialic acid (SA)]. Compared with the previous reports of FWM imaging studies,[14-16] our PE-FWM droplet imaging analysis platform is designed specifically for the single-cell analysis (**Scheme 1a**). Because of the large amount of information and multiple reference information from the data matrix of each image, the accuracy of the single-cell analysis technique based on imaging will be greatly improved and it can provide cell morphology-related information of the targets. So, single-cell imaging analysis tends to point to the cell function directly rather than the intensity-based strategy. Owing to the high

requirements of single-cell analysis, we adopted automated processing to achieve high-throughput analysis (**Scheme 1b**). By integrating many merits of microdroplets, this technique can be applied for tracking the dynamic changes of specific cells and intuitively reflect the distribution of substances on the cell surface. This technique will be promising for many single-cell analysis systems involving cytobiology, metabolites, drug metabolism, disease diagnosis and monitoring. It also lays a solid foundation for single-cell sorting based on PE-FWM imaging.

Results and Discussion

Plasmon enhancement is a local field enhancement strategy, which can serve many spectroscopic phenomena, e.g. surface-enhanced Raman scattering,[19] plasmon-enhanced fluorescence,[20] and many nonlinear optical phenomena[13-16] (**Figure S2a**) as well. In the PE-FWM process, the incidence light field strengthened by plasmon resonance will contribute remarkably to the radiative efficiency since it can amplify excitation efficiency *via* three incident photons joining in.[12,13] To assess the effect of incidence light field, the local field distribution was firstly simulated under our experimental conditions by the finite-difference time-domain simulation. A spherical AgNP (50 nm) was

chosen as a model. The third-order nonlinear susceptibility $\chi^{(3)}$ of Ag is 2.6×10^{-9} esu.[21] Under three beams (two of 790 nm as pump light, and one of 1031 nm as probed light, see **Figure S2a**), the FWM signal will be excited, which produces a peak at the wavelength of 640.78 nm (**Figure S2c**), proving that the signal achieved is the FWM signal according to the frequency calculation. **Figure S2c** displays the AgNP shows a strong local electric field at two sides of the Ag particle. The simulation results prove that the spherical AgNP is an outstanding candidate as an excellent signal reporter in FWM imaging.

Two PE-FWM nanoprobes, Ag@anti-EGFR and Ag@MPBA, were designed by coating AgNPs (**Figure S1a**) with (anti-EGFR, 116) (**Scheme S1a**) and 4-mercaptophenylboronic acid (MPBA) (Scheme S1b), which can recognize EGFR by immune mechanism[17] or identify SA by molecular identification.[18] With the assistance of these nanoprobes, we can evaluate EGFR and SA on the single living cell membrane by using the FWM effect of AgNPs.

The dark-field imaging was first performed to confirm the binding of nanoprobes based on the strong plasmonic scattering effect of AgNPs. **Figure 1a** (1)-(3) show the dark-field images of LO2 cells decorated with Ag@MPBA in three droplets. It can be observed that

many nanoprobes are collected on the cell surface. However, the bright boundaries of droplets are well-marked under these dark-field images, which will bring interferences for identifying AgNPs in the image

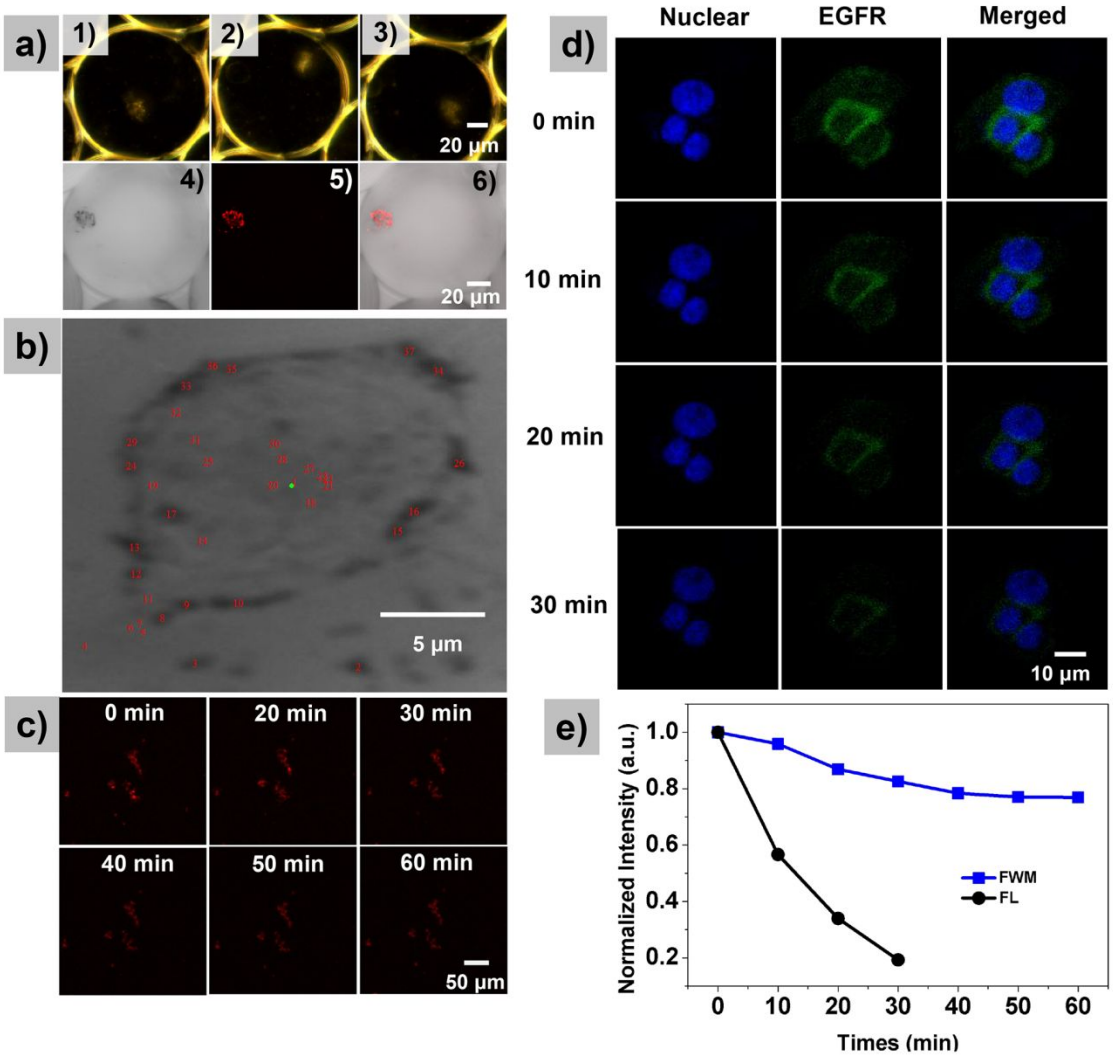

Figure 1. a) (1)-(3) Dark-field images of the Ag@MPBA binding with SA on the single LO2 cell surface. (4)-(6) Bright-field, FWM and overlay images of Ag@MPBA binding with SA on the single HepG2 cell surface. b) Optical image processing with "Partical Finder" of LabSpec6 software. Red numbers point out identifiable particles and 37 particles are marked on this image. c) The FWM imaging of AgNPs from 0 min to 60 min. d) Nuclear, EGFR, merged fluorescence imaging of HepG2 cell from 0 min to 30 min. e) Diagram of the normalized intensity of the FWM signal of AgNPs and the fluorescence signal of EGFR over time under laser continuous scanning.

processing step. Also, owing to recording the images in a liquid phase, these nanoprobes are hard to identify one by one due to light refraction in liquid. Interestingly, these interferences from stray light or droplets can be completely avoided under FWM imaging. As shown in **Figure 1a** (4)-(5), the AgNPs-based nanoprobes on the single-cell surface are clearly identified and they provide a high image contrast relative to the droplets and their environments. In comparison to bright-field imaging of the nanoprobe on a single HeLa cell (**Figure 1b**), only a few Ag@MPBA nanoprobes (Particle 1 to 37) with relatively

large size (displaying darker) can be recognized by using an automatic particle search function named as “Particle Finder” in LabSpec6 software (HORIBA, France), indicating these bright-field images also give a relatively low sharpness so that lots of nanoprobes can’t be automatically recognized during image processing. Therefore, a high-contrast image is essential for an imaging-based method and our PE-FWM can satisfy this high requirement on the image contrast (**Figure 1a** (5)).

The anti-fade property of AgNPs in FWM imaging is prominent in comparison with the commercial dyes used for confocal fluorescence imaging. **Figure 1c** shows the FWM images of AgNPs under continuous laser scanning (0 to 60 min, 7.0 mW). The signal strength is strongest at the beginning (0 min) due to the superposition of FWM and two-photon luminescence (TPL) of the nanoparticles (**Figure S7**).[14] With the continuous scanning of the laser, the two-photon fluorescence gradually quenched, and the FWM signal eventually reached a steady-state (over 30 min). For comparison, the fluorescent imaging quality under long-term irradiation (*via* a FV1000 confocal fluorescence microscope with an excitation wavelength of 488 nm and a laser power of less than 3 mW) was assessed by using a commercial fluorescent dye (Alexa Fluor 488 dye) labeled

donkey anti-mouse IgG (H+L) tracer (targeting EGFR on the cell surface with the bridge of anti-EGFR). It can be observed from **Figure 1d** that the fluorescence gradually fades with the continuous laser scanning. Intensity decays along with the laser irradiation time (**Figure 1e**) clearly show that the FWM signal of AgNPs can stand for long-period laser scanning, which is beyond commercial fluorescence dyes and is applicable for monitoring cell dynamics as long as hours. MNPs show anti-fade capability is mainly because the hot carriers excited of MNPs can give multiple outcomes on their photoemission (e.g. the ejection or fast internal relaxation of hot carriers, the production of strong optical near fields and/or the (re-)emission of a photon[22]) and all these processes are benefited from large light collection efficiency of MNPs, making them surpasses most fluorescent dyes.

To verify the performance of AgNPs in the PE-FWM imaging, we selected three cell lines (HepG2 and HeLa as the cancer cell lines and LO2 as the normal cell line) to visualize their SA expressions by a SA-specific nanoprobe. By culturing these cells with Ag@MPBA, we isolated cells in droplets. The FWM images of three kinds of cells in droplet arrays were taken (1024 ×1024 pixel, 636×636 μm, 20.97 s/frame, **Figure S8a**). It should note that the laser power for imaging was 7.0 mW, which is much lower than other

FWM imaging used for cell imaging, e.g. 150 mW in literature.[23] A low excitation laser power can suppress the fluorescent interferences from substances.[24] As can be seen from Figure S8a and 2a, the droplets, surfactant, cell itself, and poly(dimethylsiloxane) microchip, etc. has no background interference.

Image J software was used to automatically calculate the integrated density of adsorbed AgNPs on single cells in droplets. Cells with brightness over a threshold were counted. Subsequently, the Integrated Density values (IntDen) of 202 groups for three cell lines were respectively presented and dealt with T-test (**Figure S8b** and **S8c**). We can observe that HepG2 and HeLa cells both show a higher SA level than LO2 cells (p<0.001), in which HepG2 gives the highest. These data prove the PE-FWM imaging combined with the microdroplet array is a feasible way for determining targets or receptors on the cell membranes and further revealing cell heterogeneity at the single-cell level.

Next, we evaluated EGFR, another biomarker expressed on the cell membrane, to further verify the feasibility of FWM imaging for the microdroplet-based single-cell analysis. Conventional techniques for EGFR detection include enzyme-linked immunosorbent assay (ELISA), western blotting, and Immuno Histochemistry.[25] ELISA is still the golden

standard for studying protein concentrations, however, it is a time-consuming method (needs 5~6 h). Here, a simple detection method based on the PE-FWM effect of an EGFR-specific Ag nanoprobe (Scheme S1) was developed. We can achieve high-throughput detection of EGFR at the single living cell level, and the sample preparation time is only 1.5 h (Nanoprobe incubation with cells for 1 h, cell suspension preparation for 15 min, droplet preparation for 15 min). **Figure 2a** shows EGFR expressions on isolated individual cells from three different cell lines revealed by the PE-FWM imaging. The EGFR expression levels determined by IntDen show significantly different among the three cell lines ($p<0.001$). The amounts of Ag@anti-EGFR on HepG2 and HeLa cells are much higher than that of LO2, proving again the over-expression of EGFR on cancer cell lines (**Figure 2b**). Heterogeneity between cells is also verified by the heatmap (**Figure 2c**).

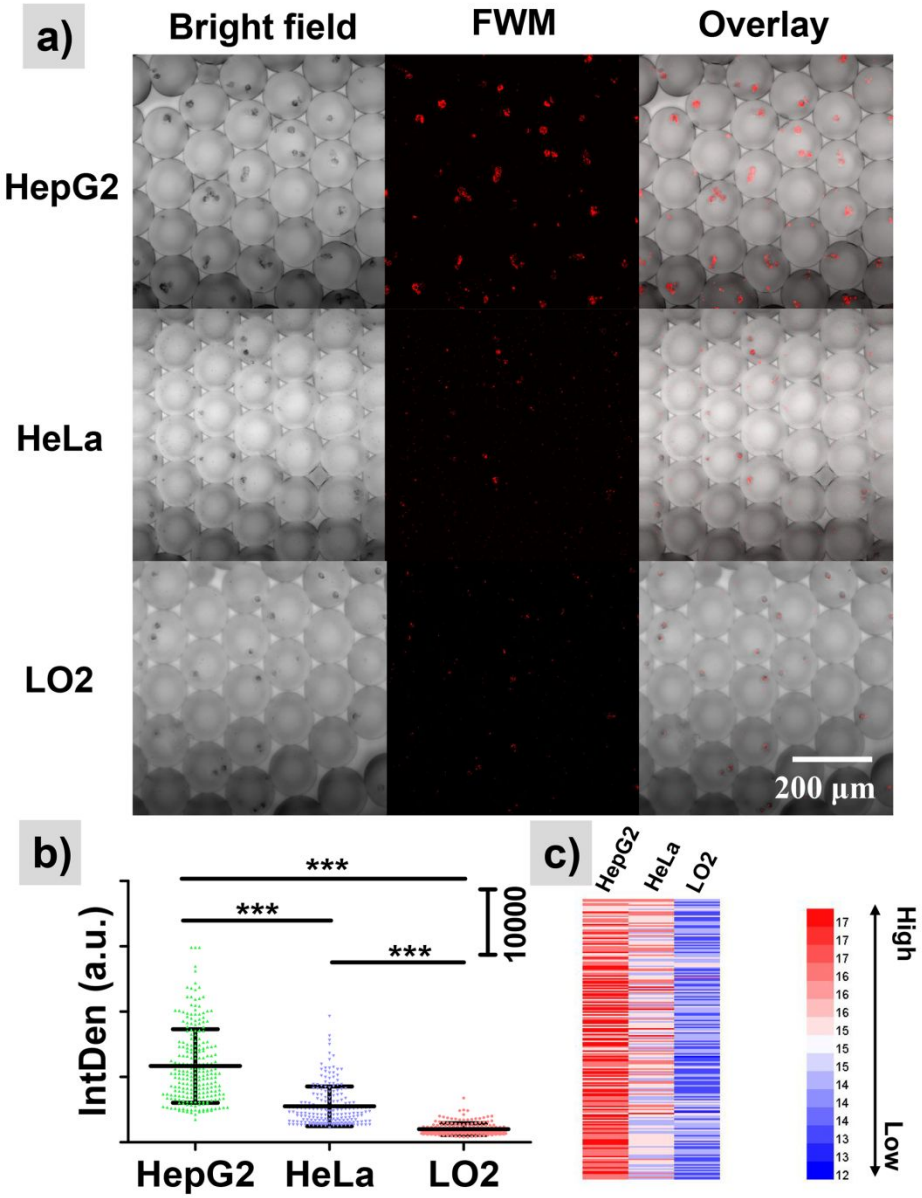

Figure 2 (a) The bright-field, FMW and overlaid images of the Ag@anti-EGFR nanoprobe on HepG2, HeLa and LO2 cells in microdroplet arrays, respectively. (b) T-test analysis of the IntDen of EGFR from each cell line. 202 groups of cells on each cell line processed with Image J software (National Institutes of Health) are plotted. The error bars represent

the standard deviations of mean IntDen. (c) Heatmap of EGFR from three cell lines. *** means significantly different at the p-value<0.001.

Conclusions

In conclusion, a high-throughput PE-FWM imaging-microdroplet platform was established successfully to realize the detection of biomarkers on the cell surface at single living cell levels. Cell heterogeneity is revealed according to the over-expressions of EGFR and SA on different cancer cell lines. This PE-FWM imaging features high imaging sensitivity and excellent imaging contrast superior to many other optical imaging methods, e.g. dark-field and bright-field images, which improves accuracy in automatic recognition during image processing. Photobleaching effect, which is commonly observed in confocal fluorescence imaging, can be avoided to a certain degree. The upconversion feature can avoid spontaneous luminescence of biosamples. Thus, this method is an excellent candidate for real-time single-molecule imaging, single-cell analysis, bioimaging, metabolite, and drug imaging by developing MNP-based nanoprobes.

ASSOCIATED CONTENT

Supporting Information. The following files are available free of charge. Reagents, synthesis of nanoprobe, electromagnetic field distribution of AgNP under FMW, single-cell encapsulation in droplets, dark-field imaging and bright-field imaging (particle-finder), fluorescence imaging of EGFR on cell surface, the FWM and TPL intensity of AgNPs, FWM imaging of single cell contained droplet array and automatic image processing by Image J (PDF).

AUTHOR INFORMATION

Corresponding Author

*E-mail: xusp@jlu.edu.cn (S. X.).

ORCID

Weiqing Xu: 0000-0002-1947-317X

Yuling Wang: 0000-0003-3627-7397

Shuping Xu: 0000-0002-6216-6175

Notes

The authors declare no competing financial interests.

ACKNOWLEDGMENT

This work was supported by National Natural Science Foundation of China (Grant No. 21873039, 21573087, and 21573092) and the grant of China Scholarship Council. We are grateful of Prof. Wei Shi, Key Lab for Molecular Enzymology & Engineering of Ministry of Education, for using cell culture room.

REFERENCES

(1) Chien, J. C.; Ameri, A.; Yeh, E. C.; Killilea, A. N.; Anwar, M.; Niknejad, A. M. A High-Throughput Flow Cytometry-on-a-CMOS Platform for Single-Cell Dielectric Spectroscopy at Microwave Frequencies. *Lab Chip.* **2018,** *18* (14), 2065-2076.

(2) Joensson, H. N.; Andersson Svahn, H. Droplet Microfluidics-a Tool for Single-Cell Analysis. *Angew. Chem., Int. Ed. Engl.* **2012,** *51* (49), 12176-92.

(3) Jing, T.; Lai, Z.; Wu, L.; Han, J.; Lim, C. T.; Chen, C. H. Single Cell Analysis of Leukocyte Protease Activity Using Integrated Continuous-Flow Microfluidics. *Anal. Chem.* **2016,** *88* (23), 11750-11757.

(4) Wen, N.; Zhao, Z.; Fan, B.; Chen, D.; Men, D.; Wang, J.; Chen, J. Development of Droplet Microfluidics Enabling High-Throughput Single-Cell Analysis. *Molecules.* **2016,** *21* (7).

(5) Wang, X.; Ma, Y.; Zhao, M.; Zhou, M.; Xiao, Y.; Sun, Z.; Tong, L. Determination of Glucose in Human Stomach Cancer Cell Extracts and Single Cells by Capillary Electrophoresis with a Micro-biosensor. *J Chromatogr A.* **2016,** *1469*, 128-134.

(6) Koster, S.; Angile, F. E.; Duan, H.; Agresti, J. J.; Wintner, A.; Schmitz, C.; Rowat, A. C.; Merten, C. A.; Pisignano, D.; Griffiths, A. D.; Weitz, D. A. Drop-Based Microfluidic Devices for Encapsulation of Single Cells. *Lab Chip.* **2008,** *8* (7), 1110-1115.

(7) Ji, M.; Orringer, D. A.; Freudiger, C. W. Rapid, Label-Free Detection of Brain Tumors with Stimulated Raman Scattering Microscopy. *Science Translational Medicine.* **2013,** *5*(201), 201ra119–201ra119.

(8) Zhang, C.; Huang, K. C.; Rajwa, B.; Cheng, J. X. Stimulated Raman scattering flow cytometry for label-free single-particle analysis. *Optica.* **2017**, *4*(1), 103-109.

(9) Mikami, H.; Lei, C.; Nitta, N.; Sugimura, T.; Ito, T.; Ozeki, Y.; Goda, K. High-Speed Imaging Meets Single-Cell Analysis. *Chem.* **2018,** *4* (10), 2278-2300.

(10) Willner, M. R.; McMillan, K. S.; Graham, D.; Vikesland, P. J.; Zagnoni, M. Surface-Enhanced Raman Scattering Based Microfluidics for Single-Cell Analysis. *Anal. Chem.* **2018,** *90* (20), 12004-12010.

(11) Wu, L.; Sedgwick, A. C.; Sun, X.; Bull, S. D.; He, X. P.; James, T. D. Reaction-Based Fluorescent Probes for the Detection and Imaging of Reactive Oxygen, Nitrogen, and Sulfur Species. *Acc. Chem. Res.* **2019,** *52* (9), 2582-2597.

(12) Wang, Y.; Lin, C.-Y.; Nikolaenko, A.; Raghunathan, V.; Potma, E. O. Four-Wave Mixing Microscopy of Nanostructures. *Adv. Opt. Photonics.* **2010,** *3* (1), 1.

(13) Chemla, D. S.; Heritage, J. P.; Liao, P. F.; Isaacs, E. D. Enhanced Four-Wave Mixing from Silver Particles. *Phys. Rev. B.* **1983,** *27* (8), 4553-4558.

(14) Jung, Y.; Chen, H.; Tong, L.; Cheng, J. X. Imaging Gold Nanorods by Plasmon-Resonance-Enhanced Four Wave Mixing. *J. Phys. Chem. C.* **2009,** *113* (7), 2657-2663.

(15) Masia, F.; Langbein, W.; Watson, P.; Borri, P. Triply Surface-Plasmon Resonant Four-Wave Mixing Imaging of Gold Nanoparticles. *Proc. of. SPIE.* **2011,** *7911*.

(16) Garrett, N.; Whiteman, M.; Moger, J. Imaging the Uptake of Gold Nanoshells in Live Cells Using Plasmon Resonance Enhanced Four Wave Mixing Microscopy. *Opt. Express.* **2011,** *19* (18), 17563-17574.

(17) Vasudev, A.; Kaushik, A.; Bhansali, S. Electrochemical Immunosensor for Label Free Epidermal Growth Factor Receptor (EGFR) Detection. *Biosens. Bioelectron.* **2013,** *39* (1), 300-305.

(18) Djanashvili, K.; Frullano, L.; Peters, J. A. Molecular Recognition of Sialic Acid end Groups by Phenylboronates. *Chem. Eur. J.* **2005,** *11* (13), 4010-4018.

(19) Moskovits, M. Surface-enhanced spectroscopy. *Rev. Mod. Phys.* **1985,** *57* (3), 783-826.

(20) Kadir, A.; Chris, D. G. *Metal-Enhanced Fluorescence*, *Vol. 2*, *John Wiley &Sons. Inc*, **2010**, pp. 139-160.

(21) Boltaev, G. S.; Ganeev, R. A.; Krishnendu, P. S.; Maurya, S. K.; Redkin, P. V.; Rao, K. S.; Zhang, K.; Guo, C. L. Strong Third-Order Optical Nonlinearities of Ag Nanoparticles Synthesized by Laser Ablation of Bulk Silver in Water and Air. *Appl. Phys. A.* **2018,** *124* (11), 766-780.

(22) Brongersma, M. L.; Halas, N. J.; Nordlander, P. Plasmon-Induced Hot Carrier Science and Technology. *Nat. Nanotech.* **2015,** *10* (1), 25-34.

(23) Ji, M. B.; Orringer, D. A.; Freudiger, C. W. Rapid, Label-Free Detection of Brain Tumors with Stimulated Raman Scattering Microscopy. *Sci Transl Med*. **2013,** *5* (201), 201ra119.

(24) Zumbusch, A.; Holtom, G. R.; Xie, X. S. Three-Dimensional Vibrational Imaging by Coherent Anti-Stokes Raman Scattering. *Phys. Rev. Lett*. **1999,** *82* (20), 4142-4145.

(25) Thariat, J.; Etienne-Grimaldi, M. C.; Grall, D.; Bensadoun, R. J.; Cayre, A.; Penault-Llorca, F.; Veracini, L.; Francoual, M.; Formento, J. L.; Dassonville, O.; De Raucourt, D.; Geoffrois, L.; Giraud, P.; Racadot, S.; Moriniere, S.; Milano, G.; Van Obberghen-Schilling, E. Epidermal Growth Factor Receptor Protein Detection in

Head and Neck Cancer Patients: a Many-Faceted Picture. *Clin. Cancer Res.* **2012,** *18* (5), 1313-1322.

TOC GRAPHICS

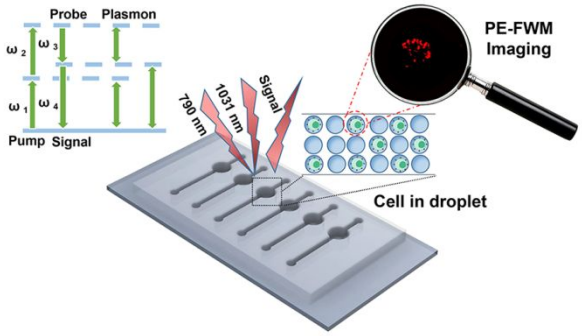

A high-throughput single-cell analytical technique is described based on the microdroplet array integrated with plasmon-enhanced four-wave mixing (PE-FWM) imaging.